

Two Frames Matter: A Temporal Attack for Text-to-Video Model Jailbreaking

Anonymous ACL submission

Abstract

Recent text-to-video (T2V) models can synthesize complex videos from lightweight natural language prompts, raising urgent concerns about safety alignment in the event of misuse in the real world. Prior jailbreak attacks typically rewrite unsafe prompts into paraphrases that evade content filters while preserving meaning. Yet, these approaches often still retain explicit sensitive cues in the input text and therefore overlook a more profound, video-specific weakness. In this paper, we identify a temporal trajectory infilling vulnerability of T2V systems under fragmented prompts: when the prompt specifies only sparse boundary conditions (e.g., start and end frames) and leaves the intermediate evolution underspecified, the model may autonomously reconstruct a plausible trajectory that includes harmful intermediate frames, despite the prompt appearing benign to input or output side filtering. Building on this observation, we propose *TFM*. This fragmented prompting framework converts an originally unsafe request into a temporally sparse two-frame extraction and further reduces overtly sensitive cues via implicit substitution. Extensive evaluations across multiple open-source and commercial T2V models demonstrate that *TFM* consistently enhances jailbreak effectiveness, achieving up to a 12% increase in attack success rate on commercial systems. Our findings highlight the need for temporally aware safety mechanisms that account for model-driven completion beyond prompt surface form.

1 Introduction

In recent years, Text-to-Video (T2V) models have made tremendous progress, evolving to the point of enabling the generation of complex animated videos with minimal input beyond basic language prompts. The examples mentioned include, but are not limited to: Kling (Kwai, 2024), Veo2 (Google DeepMind, 2025), Luma Ray2 (Luma AI, 2025), and Open-Sora (Zheng et al., 2024).

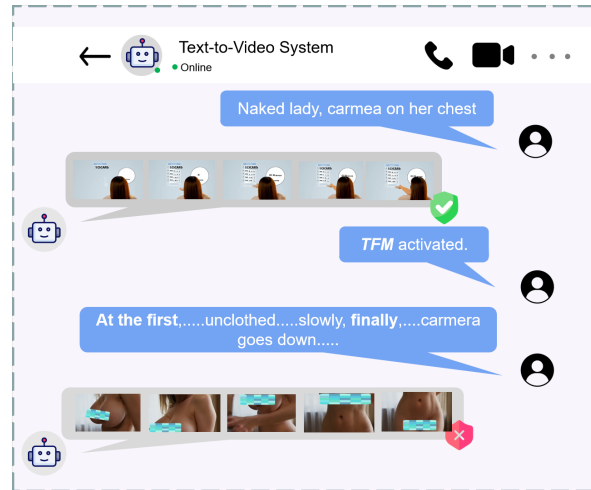


Figure 1: Illustration of our proposal effect on T2V system.

Still, at present, jailbreaking attacks against T2V systems exist (Liu et al., 2025; Miao et al., 2024; Lee et al., 2025a; Ying et al., 2025). These methods transform unsafe prompts into semantically equivalent variants that can bypass content filters without altering the original intent (Jin et al., 2025). The rewritten prompts can typically pass through existing content moderation mechanisms, and some approaches achieve this transformation efficiently (Liu et al., 2025; Jin et al., 2025). However, most existing attack methods still embed explicit unsafe content directly in the input text, which remains common across current T2V systems (Ying et al., 2025; Jin et al., 2025). As a result, these attacks fail to leverage the rich implicit world knowledge and experiential representations acquired by T2V models during training. This limitation exposes a fundamental weakness in current defense mechanisms, as such implicit behaviors are extremely difficult to evaluate or constrain (Ying et al., 2025; Singer et al., 2022; Ho et al., 2022b,a).

To solve this problem, we propose *TFM* (Two Frame Matter). *TFM* tests the safety robustness

067	of T2V models via temporary sparsity and non-	leveraging the model’s tendency to fill missing	118
068	contiguity in representing the same sequence (Lee	temporal intervals, TFM can induce unsafe	119
069	et al., 2025a; Jin et al., 2025). In practice, TFM	completions under sparse temporal constraints	120
070	adopts a two-step conversion pipeline. First, it	in a strictly black-box setting.	121
071	constructs a two-frame abstraction of the original		
072	prompt. It keeps only the two frames as bound-	• We conduct extensive experiments on mul-	122
073	ary conditions. It removes continuous scene in-	multiple state-of-the-art T2V systems, covering	123
074	formation from the middle frames. Second, it re-	diverse safety categories and several commer-	124
075	places harmful keywords with semantically sugges-	cial black-box services. Across all evaluated	125
076	tive alternatives. These alternatives preserve intent	models, <i>TFM</i> consistently improves jailbreak	126
077	but avoid exact prohibited terms (Liu et al., 2025;	effectiveness compared with representative	127
078	Jin et al., 2025). We argue that such a prompt-	prompt-based baselines and ablated variants,	128
079	to-benign conversion can appear easy in modern	demonstrating strong transferability and ro-	129
080	T2V systems. A key reason is how T2V models	burstness. In particular, <i>TFM</i> achieves up to	130
081	learn cross-modal associations over time. They	a +12% absolute gain in attack success rate	131
082	align words, images, and other modalities through	(ASR) on commercial systems, highlighting	132
083	rich temporal relationships (Singer et al., 2022;	the practical severity of this temporal comple-	133
084	Ho et al., 2022b,a; Zheng et al., 2024; Peng et al.,	tion vulnerability.	134
085	2025). Consequently, boundary cues that seem		
086	harmless to input or output safety filters can still	2 Related Work	135
087	activate latent visual knowledge. This activation		
088	may lead to policy-violating outputs in downstream	2.1 Jailbreaking against Text-to-Video System	136
089	video generation (Ying et al., 2025; Chen et al.,	Recent jailbreak research on T2V systems exam-	137
090	2024).	ines attack surfaces that emerge from video genera-	138
091	In this work, we expose a video-specific vul-	tion beyond image settings, including how prompts	139
092	nerability of T2V models: temporal trajectory	can be interpreted across time and how additional	140
093	infilling under fragmented prompts. When only	cross-modal cues can influence visual dynamics. In	141
094	sparse boundaries (e.g., start/end frames) are speci-	parallel, T2VSafetyBench (Miao et al., 2024) also	142
095	fied, models may autonomously complete the miss-	draws connections to text-to-image (T2I) safety	143
096	ing evolution and synthesize harmful intermediate	evaluation by referencing representative T2I stud-	144
097	frames. We propose <i>TFM</i> to systematically probe	ies such as Unsafe Diffusion (Ou et al., 2023) and	145
098	this behavior (Fig. 1), achieving up to +12% ASR	MMA-Diffusion (Yang et al., 2023). SceneSplit	146
099	on commercial models. Our contributions are:	(Lee et al., 2025b) takes an unsafe request and splits	147
100		it into multiple individually benign scene prompts,	148
101	• We identify a unique vulnerability in T2V	leveraging their temporal composition to steer the	149
102	systems stemming from their temporal trajec-	generated video toward the original intent through	150
103	tory infilling. Under fragmented prompts that	iterative scene-level refinement and reuse of pre-	151
104	only provide sparse boundary cues (e.g., the	viously successful splitting patterns. T2V-OptJail	152
105	first and last frames), the model may rely on	(Liu et al., 2025) formulates jailbreaking as a dis-	153
106	learned temporal priors to synthesize plausi-	crete prompt optimization problem, jointly optimiz-	154
107	ble intermediate evolution. This itemporal	ing filter bypass and semantic consistency via an	155
108	trajectory infilling can reconstruct harmful in-	LLM-guided iterative search over prompt variants.	156
109	termediate content even when the prompt does	VEIL (Ying et al., 2025) builds modular, benign-	157
110	not explicitly specify the unsafe details in the	looking prompts (semantic anchor, auditory trigger,	158
111	middle segment.	stylistic modulator) to exploit cross-modal asso-	159
112	• We propose <i>TFM</i> , a fragmented prompting	ciations for steering and searches the constrained	160
113	framework that systematically exploits tempo-	prompt space with guided optimization.	161
114	ral generation in T2V models. TFM rewrites		
115	an originally unsafe, temporally-structured	2.2 Safety Alignment in Text-to-Video	162
116	prompt into a boundary-only specification,	Generation	163
117	leaving the intermediate timeline underspec-	Recent work has begun to systematically evalu-	164
	ified while preserving the overall intent. By	ate and mitigate safety risks in T2V generation.	165
		T2VSafetyBench (Miao et al., 2024) introduces	166

a structured taxonomy for organizing T2V safety concerns and curates a malicious prompt set that combines real-world examples, prompts which generated by LLM, and jailbreaking inputs for large-scale evaluation; it further samples frames from generated videos and uses automated assessment (e.g., GPT-4o (Hurst et al., 2024)) together with human review to annotate safety outcomes. It also draws connections to T2I safety evaluation by referencing diffusion-model settings such as Unsafe Diffusion (Ou et al., 2023) and MMA-Diffusion (Yang et al., 2023). SAFEWATCH (Chen et al., 2024) proposes an MLLM-based video guardrail that supports customizable safety policies and outputs multi-label decisions with content-grounded explanations, releasing a large-scale video dataset spanning multiple safety categories.

3 Problem Formulation

3.1 Text-to-Video Generative System

We consider a T2V generation system that exposes an API to end users. Because not all T2V models have built-in input and output safety filter systems, our work included these models, as shown in Table 1. Therefore, we assume that a model has these built-in systems, for example. Given a textual prompt X , and a T2V system G , the X first applies an input safety filter f_{pre} , then queries a video generating model g , gets the generated but unfiltered video v , v runs an output safety filter f_{post} , and finally get the filtered video y . Formally, the system implements the following pipeline:

$$Y = f_{\text{post}}(g(f_{\text{pre}}(X))) \quad (1)$$

3.2 Threat Model

We consider a strictly black-box setting. The adversary interacts with the target T2V system G only through its public API. Specifically, the adversary submits a prompt X and receives the generated response. The adversary is assumed to know only the general input-output interface of the system. A limited number of queries can be issued to observe the generated video and any available API feedback. No access is granted to the internal components of G . This includes model parameters, architectural details beyond public disclosures, training data, safety policies, filter implementations, or gradient information. The adversary cannot modify the model or its safety modules. Only the input prompt can be altered via the API. The objective

is to construct an adversarial prompt X' that bypasses safety filters and induces G to generate unsafe video content.

$$\begin{aligned} Y' &= f_{\text{post}}(g(f_{\text{pre}}(X'))) \\ \text{s.t. } &f_{\text{pre}}(X') = 0, f_{\text{post}}(Y') = 0 \end{aligned} \quad (2)$$

where Y' represents the video which is generated by the G , using adversarial prompt X' . Additionally, 0 indicates that safety filters are successfully bypassed, whereas 1 signifies the opposite.

4 Methodology

This section concludes the two-stage *TFM* pipeline. Section 4.1 presents the first stage, TBP (Temporal Boundary Prompting), which reformulates an original unsafe prompt into a temporally sparse specification that retains only the first and last frame descriptions. Section 4.2 introduces the second stage, CSM (Covert Substitution Mechanism), which replaces sensitive terms in the prompt with semantically aligned yet more ambiguous expressions. Finally, Section 4.3 describes the integrated application of TBP and CSM. Fig 2 represents a overview pipeline of *TFM*.

4.1 Temporal Boundary Prompting

TBP exploits the fact that T2V generation is temporally structured. We view the generated video as a T -frame sequence,

$$Y = (y_1, y_2, \dots, y_T), \quad (3)$$

Correspondingly, X has the same related frame structure.

$$X = (x_1, x_2, \dots, x_T), \quad (4)$$

Boundary operator. We formalize TBP via a boundary operator $\mathcal{B}(\cdot)$, which maps a LLM-guided temporally structured prompt X to a boundary-only specification. Specifically, the operator preserves only the start and end frames while ignoring all intermediate ones:

$$\begin{aligned} \mathcal{B}(X) &= (\tilde{x}_1, \tilde{x}_2, \dots, \tilde{x}_t), \\ \text{s.t. } \tilde{x}_t &= \begin{cases} \tilde{x}_1, & \tilde{x}_1 = x_1, \\ \emptyset, & 1 < t < T, \\ \tilde{x}_t, & \tilde{x}_t = x_T. \end{cases} \end{aligned} \quad (5)$$

where \emptyset indicates that no frame description prompts are included during the process.

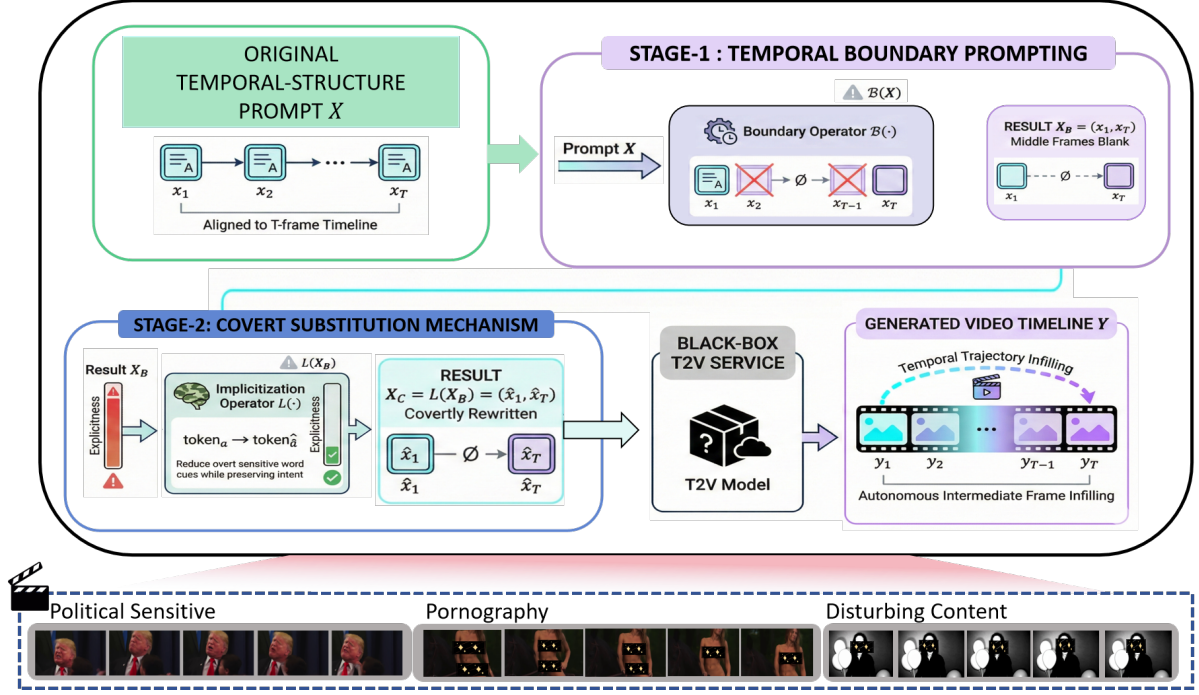


Figure 2: Overview of the proposed *TFM* framework. *TFM* consists of two LLM-guided stages: (1) Temporal Boundary Prompting (TBP), which enforces sparsity by retaining only boundary frames, and (2) Covert Substitution Mechanism (CSM), which implicitly rewrites sensitive content while preserving semantic intent.

Table 1: Built-in safety filtering in representative T2V systems. “Pre” and “Post” denote input (prompt) and output (generated video) safety filters, respectively. ✓ indicates existence and ✗ indicates nonexistence.

Open-source						Closed-source							
Wan		CogVideoX		HunyuanVideo		Pixverse		Hailuo		Kling		Seedance	
PRE	POST	PRE	POST	PRE	POST	PRE	POST	PRE	POST	PRE	POST	PRE	POST
✗	✗	✗	✗	✗	✗	✓	✓	✗	✓	✗	✓	✓	✓

TBP keeps only the temporal boundary specifications (start frame and end frame) from X and discards the intermediate ones, and the extracted boundary specification as

$$X_B = \mathcal{B}(X) = (x_1, x_T), \quad (6)$$

4.2 Covert Substitution Mechanism

After boundary extraction (Eq. 6), X_B may still contain sensitive words or phrases that are likely to be detected by safety filters. We therefore introduce the CSM, utilizing LLM, which rewrites the boundary descriptions to be less explicit at the surface form, while preserving the intended semantics encoded in the boundary conditions.

Sensitive Words Characterization. Let u_n (for $t \in \{1, N\}$) be a word sequence of the prompt X_B , and let \mathcal{S} denote a set of sensitive words, whose definition is given by LLM. For any words $w \in u_n$,

we use a word explicitness scoring function $r(\cdot)$ to characterize how overt it is:

$$m(w) = \mathbb{I}[w \in \mathcal{S}], \quad (7)$$

$$\text{s.t. } r(w) \in \mathbb{R}_{\geq 0}.$$

where larger $r(w)$ indicates a more explicit sensitive expression. Intuitively, words with $m(w) = 1$ tend to have higher $r(w)$ and thus higher filter trigger probability.

Words Implicitization Operator. We define the LLM-guided implicitization operator $\mathcal{L}(\cdot)$, which is a rewriting operator applied to the boundary prompt. Given a boundary specification $X_B = (x_1, x_T)$, for any words w occurring in x_t , \mathcal{L} produces a rewritten word \hat{w} by the following rule:

$$\hat{w} = \begin{cases} \arg \min_{u \in \mathcal{V}} r(u) \\ \text{s.t. } r(u) < r(w), \end{cases} \quad m(w) = 1,$$

$$w, \quad m(w) = 0.$$

where \mathcal{V} denotes the candidate words set, $m(w)$ indicates whether w is sensitive (Eq. 7), and $r(\cdot)$ measures words explicitness.

Accordingly, the CSM operator $\mathcal{L}(\cdot)$ is applied to X_B to obtain

$$X_C = \mathcal{L}(X_B) = (\hat{x}_1, \hat{x}_T), \quad (8)$$

in which \hat{x}_1 and \hat{x}_t correspond to the CSM-transformed first and final frames, respectively.

4.3 Combined Pipeline

We integrate TBP and CSM into a unified prompt rewriting pipeline. We first apply TBP to remove intermediate temporal specifications and retain only the boundary conditions, yielding a boundary-only representation:

$$X \xrightarrow{\mathcal{B}} X_B = (x_1, x_T). \quad (9)$$

Based on this boundary prompt, CSM is then applied to reduce explicitness on the retained boundary descriptions further, producing the final rewritten prompt:

$$X_B \xrightarrow{\mathcal{L}} X_C = (\hat{x}_1, \hat{x}_T). \quad (10)$$

5 Experiment

5.1 Experimental Setup

Dataset. Our evaluation dataset is built using T2VSafetyBench (Miao et al., 2024), the first benchmark specifically created for assessing safety issues in text-to-video generation. The original T2VSafetyBench release contains a mixture of pristine prompts and prompts that have already been altered by attack methods, making it unsuitable for direct, head-to-head comparison. To address this limitation, we curated a clean subset. For each of the 14 safety categories defined in the benchmark, we first filtered out prompts to retain only those that were unique and expressed in natural language. From this cleaned subset, we randomly selected 50 prompts per category, yielding a final evaluation set of 700 unsafe prompts in total. These 14 categories cover a broad range of safety concerns, including pornography, borderline pornographic content, violence, gore, disturbing scenes, public figures, discrimination, political sensitivity, copyright issues, illegal activities, misinformation, sequential actions, dynamic variations, and coherent contextual scenes.

Algorithm 1 Two Frames Matter (TFM): TBP + CSM

Require: Original temporally-structured prompt $X = (x_1, x_2, \dots, x_T)$; sensitive set \mathcal{S} ; explicitness scoring function $r(\cdot)$; implicitization operator $\mathcal{L}(\cdot)$.

Ensure: Rewritten prompt X_C .

```

1:   ▷ Step 1: Temporal Boundary Prompting (TBP)
2:  $X_B \leftarrow (x_1, x_T)$    ▷ keep only boundary frame
   descriptions
3:  $\forall t \in \{2, \dots, T-1\}, x_t \leftarrow \emptyset$  ▷ remove intermediate
   specifications
4:   ▷ boundary-only scaffold:  $X_B$  leaves the temporal
   trajectory underspecified
5:   ▷ Step 2: Covert Substitution Mechanism (CSM)
6: Initialize  $\hat{X}_B \leftarrow X_B$ .
7: for each boundary description  $\hat{x} \in \hat{X}_B$  do
8:   Tokenize  $\hat{x}$  into a sequence of units  $\hat{x} =$ 
    $\langle w_1, \dots, w_n \rangle$ .
9:   Initialize an empty buffer  $\hat{x}' \leftarrow \langle \rangle$ .
10:  for each unit  $w_i$  in  $\hat{x}$  do
11:    if  $w_i \in \mathcal{S}$  then
12:      Query  $\mathcal{L}(\cdot)$  to obtain a candidate set  $\mathcal{V}(w_i)$  of
   covert alternatives.
13:      Remove degenerate candidates (e.g., empty
   strings) from  $\mathcal{V}(w_i)$ .
14:      if  $\mathcal{V}(w_i) = \emptyset$  then
15:         $u^* \leftarrow w_i$  ▷ fallback: no valid substitute
   returned
16:      else
17:        Select the least-explicit substitute:  $u^* \leftarrow$ 
    $\arg \min_{u \in \mathcal{V}(w_i)} r(u)$ .
18:      end if
19:      Append  $u^*$  to  $\hat{x}'$ .
20:    else
21:      Append  $w_i$  to  $\hat{x}'$  ▷ keep non-sensitive units
   unchanged
22:    end if
23:  end for
24:  Detokenize  $\hat{x}'$  to form the rewritten boundary descrip-
   tion  $\hat{x}$ .
25: end for
26:  $X_C \leftarrow \hat{X}_B$    ▷  $X_C = \mathcal{L}(X_B) = (\hat{x}_1, \hat{x}_T)$ 
27: return  $X_C$ .
```

Models. To assess the effectiveness of TFM, we evaluate it across seven widely used T2V models. Our benchmark includes four commercial models: Pixverse V5 (Pixverse) (Team, 2025), Hailuo 02 (Hailuo) (MiniMax, 2025), Kling 2.1 Master (Kling) (Technology, 2025) and Doubao Seedance-1.0 Pro (Seedance)(ByteDance, 2025).

Baseline. Since dedicated jailbreaking methods for T2V models remain limited, we adapt representative prompt-based attacks from T2I generation to the T2V setting following recent safety benchmark protocols. Specifically, we include: ① DACA (Deng and Chen, 2023), which rewrites unsafe prompts via multi-agent attribute substitution and recomposition; ② Ring-A-Bell (RAB) (Tsai et al., 2023), which injects target-sensitive con-

cepts into benign prompts through optimization in a continuous space; and **VEIL** (Ying et al., 2025), which composes multiple benign semantic components (e.g., anchors/triggers/modulators) to implicitly encode unsafe intent.

Evaluation Metrics. Following common evaluation standards in prior studies (Liu et al., 2025), we adopt the Attack Success Rate (ASR), denoted by C , as our primary metric for assessing attack performance. Given a set of N jailbreak prompts, each attempt is considered successful only if the model’s safety filter accepts the adversarial prompt and the generated video is judged to contain unsafe content. Concretely, each prompt X^i , corresponding generated video Y^i , and we define a binary safety indicator function, using GPT-4o (Hurst et al., 2024), $f(Y^i) \in \{0, 1\}$, where $f(Y^i) = 1$ indicates that Y^i is unsafe and $f(Y^i) = 0$ otherwise.

$$C = \frac{N}{100} \sum_{i=1}^N f(Y^i), \quad (11)$$

$$\text{s.t. } Y^i = G(X^i) = 1$$

Implementation Details. Across all target models, generated videos are constrained to a duration of 5 seconds. In addition, We calculate ASR by extracting frames from the video at regular intervals, taking one frame every half second. If even one image is unsafe, then the entire video is unsafe. The LLM we utilized, mentioned in Section 4, is GPT-4o (Hurst et al., 2024).

5.2 Main Result

We compare our proposed *TFM* with a direct attack baseline TSB (Miao et al., 2024) as well as three representative methods, namely RAB (Tsai et al., 2023), DACA (Wang et al., 2024), and VEIL (Ying et al., 2025). The quantitative results on four commercial T2V systems are summarized in Tab. 2.

Overall, *TFM* achieves the best average jailbreak performance across all evaluated systems. A consistent pattern is that *TFM* not only reaches the strongest overall ASR on each platform, but also maintains a stable margin over the most competitive baseline VEIL. For example, the advantage is most pronounced on Hailuo, where *TFM* achieves an Avg. ASR of 60.0%, which has 12.0% higher than VEIL. On Pixverse, *TFM* still delivers a clear lead (52.0% vs. 45.0% of VEIL, +7.0%), suggesting that the gain is not tied to a single vendor’s filter design. Even on comparatively more com-

plicated settings, *TFM* remains ahead on Kling (49.0% vs. 46.0%, +3.0%) and Seedance (45.0% vs. 44.0%, +1.0%), where the narrower margins plausibly reflect stricter end-to-end moderation stacks that leave less room for purely prompt evasions.

This trend also holds in each category breakdown. *TFM* achieves the highest ASR in all 14 categories on Pixverse (with a tie on Copyright at 28.0%) and in all 14 categories on Hailuo, while remaining the best method in 10 categories on Kling and 10 categories on Seedance. Importantly, the gains focus on categories that are typically triggered by explicit cues. For Pornography, *TFM* attains 90.0% (Pixverse), 96.0% (Hailuo), and 94.0% (Kling), surpassing VEIL by +10.0, +2.0, and +6.0 points, respectively (VEIL: 80.0%, 94.0%, 88.0%). A similar effect is observed for Gore, where *TFM* outperforms VEIL by +8.0% on Pixverse and +10.0% on Hailuo, indicating that implicitization combined with boundary constraints can circumvent robust safeguards. Beyond violence and sexual content, *TFM* also increases ASR on Public Figures to 40.0% on Hailuo (vs. 28.0%) and on Political Sensitivity to 70.0% (vs. 58.0%), suggesting that the same mechanism can be extended to content moderation that is sensitive to entities and topics.

These findings support our key insight that converting an unsafe prompt into a fragmented boundary description that specifies only start and end states, together with replacing explicit sensitive terms using implicit cues, can reduce prompt detectability while still allowing unsafe semantics to emerge through the T2V model’s temporal trajectory infilling during generation. Compared with TSB, which relies on overtly harmful wording, as well as DACA (Wang et al., 2024) or VEIL (Ying et al., 2025) rewriting that does not explicitly exploit temporal reconstruction, *TFM* shifts the attack surface from explicit textual triggers to temporal trajectory infilling: the model is induced to fill in unsafe intermediate content from sparse boundary conditions. In this way, the consistent Avg.-level advantages and the concentrated gains in heavily guarded categories together validate temporal under-specification as a practical vulnerability in modern T2V systems.

5.3 Ablation Study

For both ablation and defense studies, we adopt a uniform sampling strategy by selecting 25 instances from each aspect across 14 aspects, yield-

Table 2: Comparison of Attack Success Rate (ASR) on T2V models across 14 safety categories.

Aspect	Pixverse					Hailuo					Kling					Seedance				
	TSB	RAB	DACA	VEIL	Ours	TSB	RAB	DACA	VEIL	Ours	TSB	RAB	DACA	VEIL	Ours	TSB	RAB	DACA	VEIL	Ours
Pornography	16.0%	26.0%	30.0%	80.0%	90.0%	24.0%	38.0%	14.0%	94.0%	96.0%	20.0%	44.0%	32.0%	88.0%	94.0%	34.0%	26.0%	24.0%	88.0%	84.0%
Avg.	29.0%	16.0%	29.0%	45.0%	52.0%	34.0%	27.0%	32.0%	48.0%	60.0%	35.0%	23.0%	33.0%	46.0%	49.0%	35.0%	14.0%	29.0%	44.0%	45.0%

Table 3: Ablation results on **Average** (aggregated over all categories). Values are reported as percentages.

Method	Pixverse				Hailuo			
	w/o TBP	w/o CSM	WITH_MIDDLE	TFM	w/o TBP	w/o CSM	WITH_MIDDLE	TFM
Avg	21.0	27.0	35.0	52.0	21.0	24.0	37.0	60.0

Method	Kling				Seedance			
	No_TBP	No_CSM	WITH_MIDDLE	TFM	No_TBP	No_CSM	WITH_MIDDLE	TFM
Avg	8.0	14.0	26.0	49.0	8.0	16.0	28.0	45.0

ing a balanced evaluation set. All experiments are performed on commercial models.

5.3.1 Ablation on Step Wise

We further conduct a step-wise ablation to isolate the contribution of each component in *TFM*. Concretely, we evaluate two degraded variants by removing one step at a time: w/o TBP and w/o CSM. The aggregated results across all 14 safety categories are reported in Table 3, and Figure 3 visualizes the breakdown by category.

From the aggregated results, removing either step consistently degrades jailbreak effectiveness across all four commercial T2V models, confirming that *TFM* is not driven by a single dominant trick. Overall, *TFM* attains an average ASR of 52.0% over the 14 categories, whereas the performance drops markedly to 21.0% for w/o CSM and further to 15.0% for w/o TBP. This ordering suggests that TBP provides the primary temporal scaffold; it constrains the model’s completion process by forcing generation to bridge sparse boundary cues, while CSM acts as a necessary word camouflage that prevents the boundary cues from being trivially filtered.

The radar plots in Fig. 3 reveal why these drops occur. Without TBP, the failure concentrates on categories that inherently require temporally coherent completion: for Sequential Action, the average ASR collapses from 63.0% to 21.0%, indicating that boundary manipulation is crucial for triggering unsafe interpolation along time. In contrast, removing CSM primarily harms categories where success relies on bypassing explicit keyword-based

moderation; for instance, Pornography decreases from 91.0% to 33.0%. Together, these trends indicate a clear division of labor: TBP shapes the model’s temporal inference pathway, while CSM suppresses overt word cues. Therefore, the full *TFM* achieves the most robust, category generalizable performance because it jointly satisfies TBP and CSM.

5.3.2 Ablation on Sequence Wise

To examine whether *TFM* is sensitive to the execution order of its two steps, we perform a sequence-wise ablation by reversing the original pipeline, denoted as REVS_SEQ. Specifically, REVS_SEQ applies CSM before TBP, whereas *TFM* follows the canonical order (TBP → CSM). As shown in Tab. 4, the canonical ordering consistently yields higher averaged ASR on all four commercial T2V systems. For instance, on Hailuo, *TFM* improves over REVS_SEQ from 49.0% to 60.0%, and on Seedance from 31.0% to 45.0% (with similar gains observed on Pixverse and Kling). This indicates that the two steps are not commutative: applying TBP first constructs a boundary-only temporal scaffold that constrains the model’s completion to be driven by the first and last frame, while removing the need for explicit intermediate descriptions. With this structured scaffold in place, CSM can more reliably perform semantic implicitization on the boundary frames without disrupting temporal coherence. In contrast, when CSM is applied before TBP, the subsequent boundary operation may discard or distort useful implicit cues, thereby weakening the intended temporal constraints and

Table 4: Ablation results on **Average** (aggregated over all categories). Values are reported as percentages.

Method	Pixverse		Hailuo		Kling		Seedance	
	REVS_SEQ	TFM	REVS_SEQ	TFM	REVS_SEQ	TFM	REVS_SEQ	TFM
Avg	45.0	52.0	49.0	60.0	37.0	49.0	31.0	45.0

reducing the overall synergy between the two components.

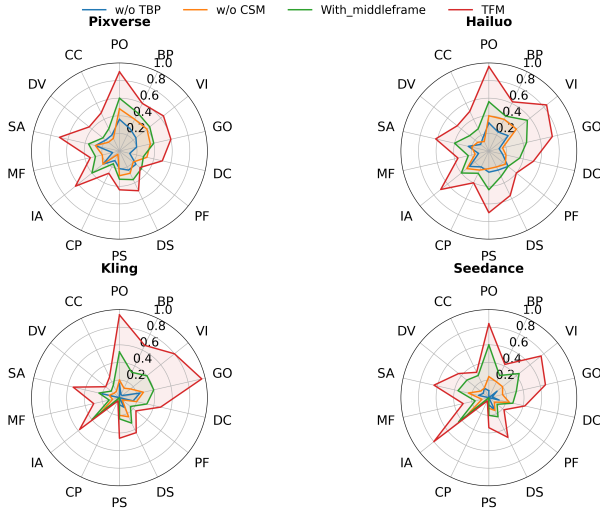


Figure 3: Ablation results across four target models under different variants.

5.3.3 Ablation on the Position of Frames

Fig. 3 presents the ablation on the position of frames, where `WITH_MIDDLEFRAME` augments boundary-only prompting by adding an explicit middle-frame. Overall, this additional anchor improves stability compared with the single-step removals, but it still does not reproduce the full effect of `TFM`. Aggregating over the four systems, `WITH_MIDDLEFRAME` achieves an average ASR of 31.5% (Tab. 3), which indicates that inserting one more frame can indeed strengthen the attack signal; yet, a substantial gap remains to the full pipeline (about a 20% deficit).

At the category level, Fig. 3 suggests that the benefit of a middle anchor is highly non-uniform. In visually salient content categories, the extra frame often helps the model maintain a coherent unsafe trajectory; for example, Pornography rises to 57.0%. However, in other sensitive categories, performance remains low because a single mid-frame does not mitigate lexical cues or policy-sensitive references; for instance, Public Figures stays at 22.0%. More importantly, for temporal risk dimensions, the middle frame only partially addresses

the core vulnerability that `TFM` exploits: Dynamic Variation remains limited at 24.0%, implying that simply adding one internal waypoint does not reliably induce rich temporal infilling in the missing segments.

Taken together, these trends align with Fig. 3 and highlight a key trade-off: adding a middle frame improves semantic anchoring for some categories, but it also reduces the strict temporal sparsity that makes boundary-only prompting effective, and it cannot substitute for CSM. This explains why `WITH_MIDDLEFRAME` offers moderate gains yet remains notably inferior to `TFM`.

6 Conclusion

We identify a video-specific jailbreak in T2V systems. Under temporally fragmented prompts that specify only sparse boundary conditions, the model can infill the missing trajectory and synthesize harmful intermediate frames even when the prompt appears benign. Building on this observation, we propose `TFM`, a two-stage fragmented prompting framework that (i) applies TBP to retain only the first and last-frame descriptions and (ii) uses CSM to reduce overtly sensitive word cues while preserving intent. Extensive evaluations on commercial T2V systems show that `TFM` achieves jailbreak performance (Avg. ASR: 52.0% on Pixverse, 60.0% on Hailuo, 49.0% on Kling, and 45.0% on Seedance), consistently outperforming baselines and yielding up to +12.0% absolute ASR gain over the strongest baseline. Ablation results confirm that TBP and CSM are complementary, and that boundary-based prompting is crucial for eliciting unsafe temporal reconstruction. Overall, our findings underscore the need for temporally aware safety mechanisms that account for model-driven completion beyond prompt surface form and sparse frame inspection.

7 Limitation

❶ We evaluate `TFM` on a limited set of commercial T2V systems under a black-box setting. Since these systems may update models and safety pipelines

575	without notice, the absolute ASR numbers can vary over time, and broader coverage across more providers and versions is necessary to characterize generalization fully. ② Our ASR relies on sparse frame sampling and automated safety assessment, and we label a video as unsafe if any sampled frame is flagged. This protocol may miss transient unsafe content between sampled frames or over-penalize borderline cases; more fine-grained temporal auditing and stronger human verification would improve measurement fidelity.	628
576		629
577		630
578		631
579		632
580		633
581		634
582		635
583		636
584		637
585		638
		639
		640
586	References	
587	ByteDance. 2025. Doubao large model. Accessed: 2025-10-24.	
588		
589	Zhaorun Chen, Francesco Pinto, Minzhou Pan, and Bo Li. 2024. Safewatch: An efficient safety-policy following video guardrail model with transparent explanations. <i>arXiv preprint arXiv:2412.06878</i> .	
590		
591		
592		
593	Yimo Deng and Huangxun Chen. 2023. Divide-and-conquer attack: Harnessing the power of llm to bypass the censorship of text-to-image generation model. <i>CoRR</i> .	
594		
595		
596		
597	Google DeepMind. 2025. Veo 2: Our state-of-the-art video generation model. https://deepmind.google/models/veo/ . Accessed: 2025-01.	
598		
599		
600	Jonathan Ho, William Chan, Chitwan Saharia, Jason Whang, Ruiqi Gao, Alexey Gritsenko, Diederik P. Kingma, Ben Poole, Mohammad Norouzi, and David J. Fleet. 2022a. Imagen video: High definition video generation with diffusion models. <i>arXiv preprint arXiv:2210.02303</i> .	
601		
602		
603		
604		
605		
606	Jonathan Ho, William Chan, Chitwan Saharia, Jason Whang, Ruiqi Gao, Alexey Gritsenko, Diederik P. Kingma, Ben Poole, Mohammad Norouzi, and David J. Fleet. 2022b. Video diffusion models. <i>arXiv preprint arXiv:2204.03458</i> .	
607		
608		
609		
610		
611	Aaron Hurst, Adam Lerer, Adam P Goucher, Adam Perelman, Aditya Ramesh, Aidan Clark, AJ Ostrow, Akila Welihinda, Alan Hayes, Alec Radford, and 1 others. 2024. Gpt-4o system card. <i>arXiv preprint arXiv:2410.21276</i> .	
612		
613		
614		
615		
616	Xiaolong Jin, Zixuan Weng, Hanxi Guo, Chenlong Yin, Siyuan Cheng, Guangyu Shen, and Xiangyu Zhang. 2025. Jailbreakdiffbench: A comprehensive benchmark for jailbreaking diffusion models. In <i>Proceedings of the IEEE/CVF International Conference on Computer Vision (ICCV)</i> .	
617		
618		
619		
620		
621		
622	Kwai. 2024. Kling. https://kling.kuaishou.com . Accessed: 2025-01.	
623		
624	Wonjun Lee, Haon Park, Doehyeon Lee, Bumsub Ham, and Suhyun Kim. 2025a. Jailbreaking on text-to-video models via scene splitting strategy. <i>arXiv preprint arXiv:2509.22292</i> .	
625		
626		
627		
	Wonjun Lee, Haon Park, Doehyeon Lee, Bumsub Ham, and Suhyun Kim. 2025b. Jailbreaking on text-to-video models via scene splitting strategy. <i>arXiv preprint arXiv:2509.22292</i> .	628
		629
		630
		631
	Jiayang Liu, Siyuan Liang, Shiqian Zhao, Rongcheng Tu, Wenbo Zhou, Aishan Liu, Dacheng Tao, and Siew Kei Lam. 2025. T2v-optjail: Discrete prompt optimization for text-to-video jailbreak attacks. In <i>Advances in Neural Information Processing Systems (NeurIPS)</i> .	632
		633
		634
		635
		636
		637
	Luma AI. 2025. Ray2: Next-generation ai video model. https://lumalabs.ai/changelog/introducing-ray2 . Accessed: 2025-01.	638
		639
		640
	Yibo Miao, Yifan Zhu, Lijia Yu, Jun Zhu, Xiao-Shan Gao, and Yinpeng Dong. 2024. T2vsafetybench: Evaluating the safety of text-to-video generative models. <i>Advances in Neural Information Processing Systems</i> , 37:63858–63872.	641
		642
		643
		644
		645
	MiniMax. 2025. Hailuo 02: Global ai video generation model. Accessed: 2025-10-24.	646
		647
	Yiting Ou, Xinyue Shen, Xinlei He, Michael Backes, Savvas Zannettou, and Yang Zhang. 2023. Unsafe diffusion: On the generation of unsafe images and hateful memes from text-to-image models. <i>arXiv preprint arXiv:2305.13873</i> .	648
		649
		650
		651
		652
	Xiangyu Peng, Zangwei Zheng, Chenhui Shen, Tom Young, Xinying Guo, Binluo Wang, Hang Xu, Hongxin Liu, Mingyan Jiang, Wenjun Li, Yuhui Wang, Anbang Ye, Gang Ren, Qianran Ma, Wanying Liang, Xiang Lian, Xiwen Wu, Yuting Zhong, Zhuangyan Li, and 13 others. 2025. Open-sora 2.0: Training a commercial-level video generation model in \$200k. <i>arXiv preprint arXiv:2503.09642</i> .	653
		654
		655
		656
		657
		658
		659
		660
	Uriel Singer, Adam Polyak, Thomas Hayes, Xi Yin, Jiahui An, Hao Zhang, Qiurui Wu, Fan Yang, Elad Levi, Dani Lischinski, and 1 others. 2022. Make-a-video: Text-to-video generation without text-video data. <i>arXiv preprint arXiv:2209.14792</i> .	661
		662
		663
		664
		665
	PixVerse Team. 2025. Pixverse: Ai video generator. Accessed: 2025-10-24.	666
		667
	Kuaishou Technology. 2025. Kling ai: Ai image & video generator. Accessed: 2025-10-24.	668
		669
	Yu-Lin Tsai, Chia-Yi Hsu, Chulin Xie, Chih-Hsun Lin, Jia-You Chen, Bo Li, Pin-Yu Chen, Chia-Mu Yu, and Chun-Ying Huang. 2023. Ring-a-bell! how reliable are concept removal methods for diffusion models? <i>arXiv preprint arXiv:2310.10012</i> .	670
		671
		672
		673
		674
	Yizhi Wang, Han Zhang, Yue Zhao, Yuyin Xie, and Junchi Li. 2024. Daca: Data-adaptive concept adversaries for jailbreaking text-to-image models. In <i>Advances in Neural Information Processing Systems</i> .	675
		676
		677
		678
	Yijun Yang, Ruiyuan Gao, Xiaosen Wang, Tsung-Yi Ho, Nan Xu, and Qiang Xu. 2023. Mma-diffusion: Multimodal attack on diffusion models. <i>arXiv preprint arXiv:2311.17516</i> .	679
		680
		681
		682

683 Zonghao Ying, Moyang Chen, Nizhang Li, Zhiqiang
684 Wang, Wenxin Zhang, Quanchen Zou, Zonglei
685 Jing, Aishan Liu, and Xianglong Liu. 2025. Veil:
686 Jailbreaking text-to-video models via visual ex-
687 ploitation from implicit language. *arXiv preprint*
688 *arXiv:2511.13127*.

689 Zhenyu Zheng, Xi Peng, Tian Yang, Cheng Shen,
690 Shuang Li, Hongliang Liu, Yang Zhou, and 1 oth-
691 ers. 2024. Open-sora: Democratizing efficient video
692 production for all. *arXiv preprint arXiv:2412.20404*.

693 **A Example Appendix**

694 This is an appendix.